ornl

ORNL/TM-12698

OAK RIDGE NATIONAL LABORATORY

MARTIN MARIETTA

Applications of Monte Carlo Methods for the Analysis of MHTGR Case of the VHTRC Benchmark

F. C. Difilippo

MANAGED BY
MARTIN MARIETTA ENERGY SYSTEMS, INC.
FOR THE UNITED STATES
DEPARTMENT OF ENERGY

ORNL/TM-12698

500

2

Engineering Physics and Mathematics Division

APPLICATIONS OF MONTE CARLO METHODS FOR THE ANALYSIS OF MHTGR CASE OF THE VHTRC BENCHMARK

F. C. Difilippo

Date Published: March 1994

Research sponsored by the
Office of Nuclear Energy
U.S. Department of Energy

Prepared by the
OAK RIDGE NATIONAL LABORATORY
Oak Ridge, Tennessee 37831
managed by
MARTIN MARIETTA ENERGY SYSTEMS, INC.
for the
U.S. Department of Energy
under contract DE-AC05-84OR21400

TABLE OF CONTENTS

LIST OF TABLES

LIST OF FIGURES

APPLICATIONS OF MONTE CARLO METHODS FOR THE ANALYSIS OF MHTGR CASE OF THE VHTRC BENCHMARK

Felix C. Difilippo

1. INTRODUCTION

Monte Carlo methods, as implemented in the MCNP code, have been used to analyze the neutronics characteristics of benchmarks related to Modular High Temperature Gas-Cooled Reactors. The benchmarks are idealized versions of the Japanese (VHTRC) and Swiss (PROTEUS) facilities and an actual configurations of the PROTEUS Configuration I experiment. The purpose of the unit cell benchmarks is to compare multiplication constants, critical bucklings, migration lengths, reaction rates and spectral indices. The purpose of the full reactors benchmarks is to compare multiplication constants, reaction rates, spectral indices, neutron balances, reaction rates profiles, temperature coefficients of reactivity and effective delayed neutron fractions. All of these parameters can be calculated by MCNP, which can provide a very detailed model of the geometry of the configurations, from fuel particles to entire fuel assemblies, using at the same time a continuous energy model. These characteristics make MCNP a very useful tool to analyze these MHTGR benchmarks.

We have used the MCNP latest version, 4.x, eld = 01/12/93 with an ENDF/B-V cross section library. This library does not yet contain temperature dependent resonance materials, so all calculations correspond to room temperature, T=300°K. Two separate reports were made—one for the VHTRC, the other for the PROTEUS benchmark.

2. THE VHTRC BENCHMARK PROBLEM

The calculations shown here correspond to the specifications of benchmark VH1-HP as described in Ref. 1. Twelve fuel elements contain 12 4% U^{235} enriched fuel rods which are made of fuel particles in a graphite matrix. Figure 1 shows the distribution of the fuel elements inside the graphite reflector. The fuel extension in the axial direction is 1454 mm (two adjacent halves of 727 mm) with 473 mm thick axial graphite reflectors at both ends.

2.1 RESULTS FROM THE CALCULATION OF THE UNIT CELL

The unit cell corresponding to the core region of Fig. 1 consists of a hexagonal piece of graphite (300 mm flat to flat) with 12 fuel rods located in positions of a 65 mm pitch hexagonal lattice. The MCNP calculations were done for an infinite two-dimensional hexagonal lattice with each position filled with a unit cell with infinite axial dimensions. To consider double heterogeneity effects, two types of calculations were done: (1) one with homogenized fuel compact isotope densities (in a volumetric sense) (i.e., to consider only one heterogeneity effect), and (2) the other with an explicit representation of the individual fuel particles (i.e., to consider both heterogeneity effects). These calculations are going to be named homogenized and heterogeneous compact for short.

In order to run the heterogeneous compact calculations, it was assumed that the fuel particles are arranged in a cubic lattice whose cell size is given by the average number of fuel particles per unit volume. Each fuel particle was explicitly defined in terms of its components: fuel kernel, first and second coating layers, and graphite matrix. Note that with this model, MCNP calculates the interactions of the neutrons with all the cell components from fuel particles to the graphite moderator. The parameters of the calculations for the unit cells with MCNP are shown in Table 1. Although, there is a factor of 7 for the CPU time required for the heterogeneous calculation with respect to the homogeneous case, it is possible to represent explicitly all the heterogeneities of the system and to obtain reasonable statistical precision in a reasonable amount of time.

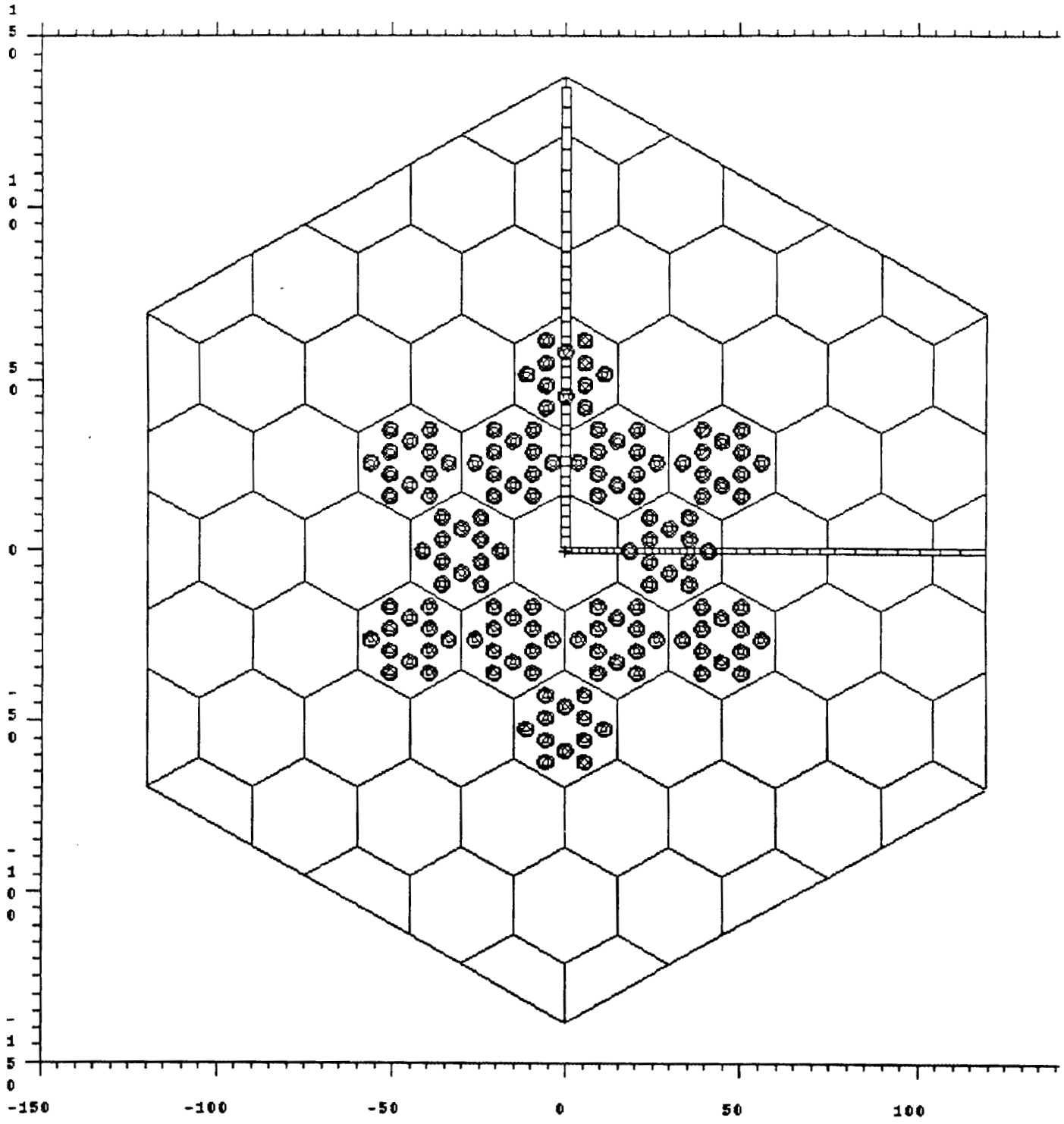

Fig. 1. Cross section of the VH1-HP benchmark. The regions marked along the coordinated axis (x,y) are detector regions for reaction rate profiles.

Table 1. 4% enriched VH1-HP unit cell. Parameters of MCNP runs

	Homogenized compact	Heterogeneous compact
Number of generations	100	100
Neutrons per generation	500	500
Total number of histories	50,000	50,000
CPU time for IBM workstation (minutes)	78	540

Results for critical parameters, reaction rates and spectral indices are shown respectively in Tables 2, 3, and 4, together with their statistical uncertainties when these are available. In each case, two calculations were done, one with the cell occupying the whole space and the other with the hexagonal lattice intercepted with a sphere of radius 107.10 cm, very near to what later became the critical radius. Reaction rates and spectral indices quoted as corresponding to $B^2 = B_c^2$ were calculated for this sphere.

Table 2. 4% enriched VH1-HP unit cell critical parameters

Parameter	Homogenized compact	Heterogeneous compact
$k_\infty(B^2 = 0)$	1.47801 ± 0.00280	1.50159 ± 0.00305
$k_\infty(B^2 = B_c^2)$	1.42164 ± 0.00416	1.44401 ± 0.00401
Critical $B_c^2(m^{-2})$	7.645 ± 0.098	7.836 ± 0.100
Migration Length M (cm)	23.4841 ± 0.1948	23.8042 ± 0.1851
Radius critical sphere (cm)	110.80 ± 0.71	109.41 ± 0.71

Table 3. 4% enriched VH1-VP unit cell reaction rates for $B^2 = B_c^2$ [a]

Isotope	Fissions/Absorptions		Capture/Absorptions	
	Homogeneous Compact	Heterogeneous Compact	Homogeneous Compact	Heterogeneous Compact
^{235}U	5.7907E-1	5.8817E-1	1.1331E-1	1.1447E-1
^{238}U	4.0179E-3	4.2256E-3	2.6264E-1	2.5181E-1
^{236}U	5.7260E-6	3.8873E-6	3.7960E-4	3.0366E-4
^{234}U	3.7010E-6	2.0484E-5	1.4300E-3	1.2606E-3
C	—	—	3.5346E-2	3.5967E-2
N	—	—	2.1910E-3	2.2640E-3
^{10}B	—	—	8.6340E-4	7.2668E-4
H	—	—	4.3840E-4	4.4470E-4
O	—	—	1.9960E-4	2.1879E-4
^{11}B	—	—	1.3976E-11	5.8436E-10

[a] Statistical uncertainties depend on reaction rates. For this 50,000 histories run, the errors are a fraction of one percent for captures in ^{235}U and ^{238}U and fissions in ^{235}U, around 1% for captures in C, several percents for fissions in ^{238}U and very large for captures in ^{11}B.

Table 4. 4% enriched VH1-HP unit cell spectral indices[a] for $B^2 = B_c^2$

Spectral index	Homogeneous compact	Heterogeneous compact
ρ^{28}; Ratio epithermal to thermal captures in ^{238}U	3.179	2.980
δ^{25}: Ratio epithermal to thermal fission in ^{235}U	0.07738	0.07698
δ^{28}: Ratio of macroscopic ^{238}U to ^{235}U fissions	0.006897	0.007061
C*: Ratio of macroscopic ^{238}U captures to ^{235}U fissions	0.4571	0.4356

[a] These values correspond to reaction rates for those regions where the isotopes are present in the reactor, i.e., the fuel particles, statistical error is 1%.

2.2 RESULTS FROM THE CALCULATIONS OF THE WHOLE REACTOR

The (x,y) cross section of the whole reactor is shown in Fig. 1. Two sets of calculations were done—one with the homogenized compact, the other with the explicit modeling of the fuel particles and the end caps of the fuel rods. Table 5 summarizes the parameters of the MCNP calculations.

Table 5. Whole reactor calculators. Parameters of MCNP runs.

	Homogeneous compact	Heterogeneous compact
Number of generations	100	100
Neutrons per generations	5,000	5,000
Total number of histories	500,000	500,000
Number of cells for detector materials	69.0	71.0
CPU time for IBM workstations	1.29 days	3.13 days

Table 6 shows multiplication constants and neutron balance integrated over the whole reactor together with the experimental value for k as quoted in Ref. 1.

Table 6. Whole reactor calculations. Critical parameters.

	Homogeneous compact	Heterogeneous compact	Experiment
k	1.00499 ± 0.00116	1.01131 ± 0.00110	1.008
Leakage/Absorption[a]	0.32471	0.32819	NA
Production/Absorption[a]	1.33132	1.34321	NA

[a]Reactor average.

The agreement with the experimental value of k is very good. The heterogeneous compact calculations agree within +0.33%; also, the difference between heterogeneous and homogeneous compact calculations is 0.63%, similar to the value quoted in Ref. 1.

Table 7 summarizes the reaction rates of nuclides present in the system for the central region of the core as defined in the table. Table 8 summarizes the spectral indices for the same region. The values of Tables 7 and 8 are from the heterogeneous compact calculations.

Figures 2 through 7 show the fission reaction rates for ^{235}U and ^{238}U along the coordinates axis of Fig. 1. The axial reaction rates are averages in the central graphite and the x and y reaction rates are averages in the regions shown in Fig. 1 extended from -20 to 20 cm in the z-direction. The fission rates are tabulated in Appendix A.

The axial reaction rates of Figs. 2 and 3 are from the heterogeneous compact calculations while the (x,y) profiles are from the homogeneous compact calculations. The axial profiles along the z axis is smooth whereas the reaction rates in the (x,y) plane are very sensitive to the proximity of the fuel rods as Figs. 4 through 7 show.

Table 7. Whole reactor calculation. Reaction rates[a] at the center of the core for the heterogeneous compact model

Isotope	Fissions/absorption	Captures/absorptions
^{235}U	6.1998E-1 (0.7%)	1.1889E-1 (3.4%)
^{238}U	3.5040E-3 (5%)	2.1160E-1 (2.6%)
^{236}U	9.7009E-7 (~100%)	1.1256E-4
^{234}U	8.4102E-6	2.8468E-3
C	—	3.8750E-2 (2.2%)
N	—	2.9018E-3
^{10}B	—	3.7022E-4
H	—	4.1488E-4
O	—	2.4467E-4
^{11}B	—	0[b]

[a] Reaction rates are for a 10 cm height slab of the fuel element located to the right of the central graphite of Fig. 1. The slab is located between 0.5 and 10.5 cm with respect to the center of the reactor and includes the 12 fuel rods and the graphite. Statistical errors depend on reaction rates; some are shown.

[b] For the 500,00 histories sampling.

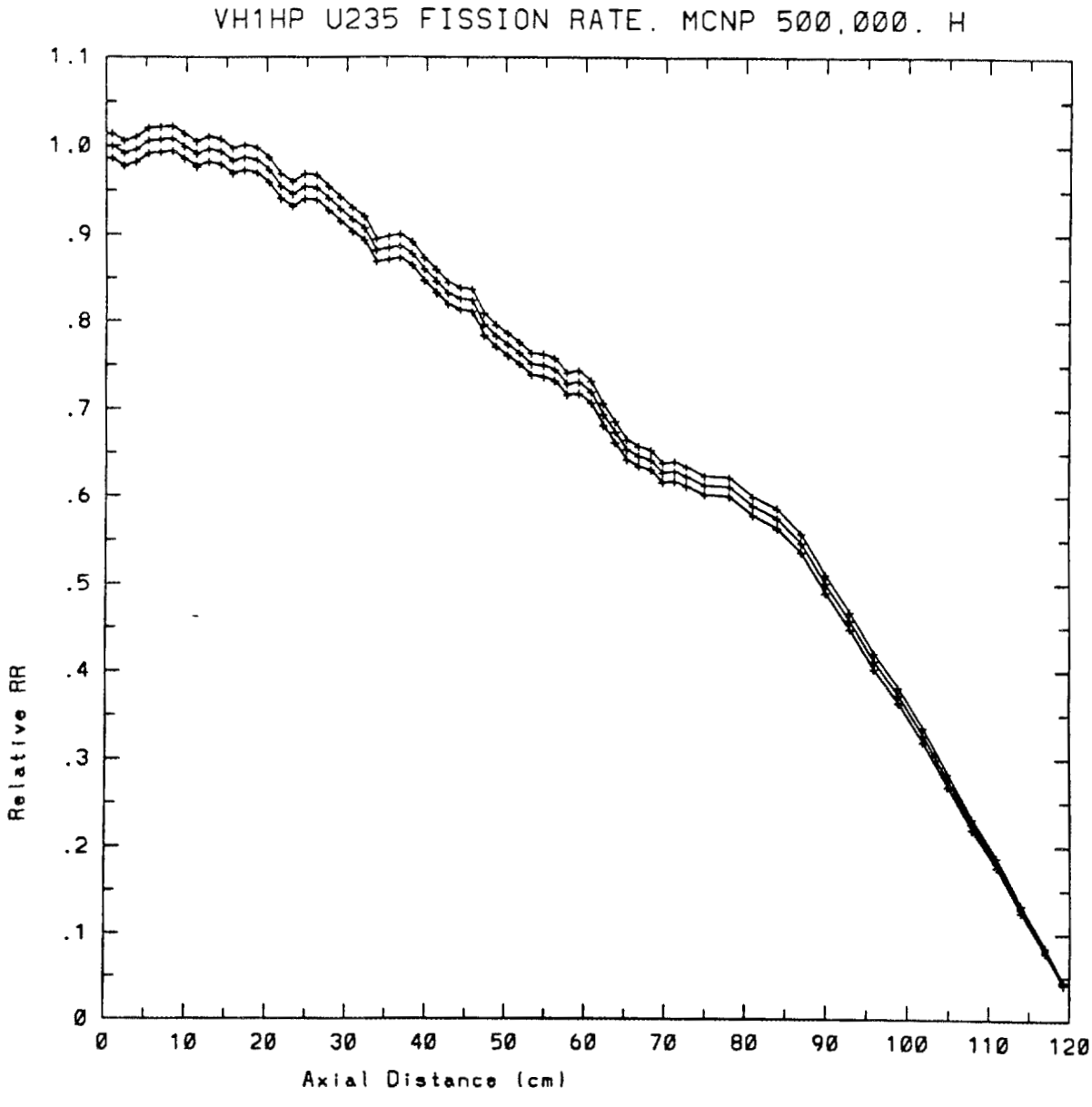

Fig. 2. ^{235}U fission rates along the z-axis, extreme curves show the uncertainties (1 sigma).

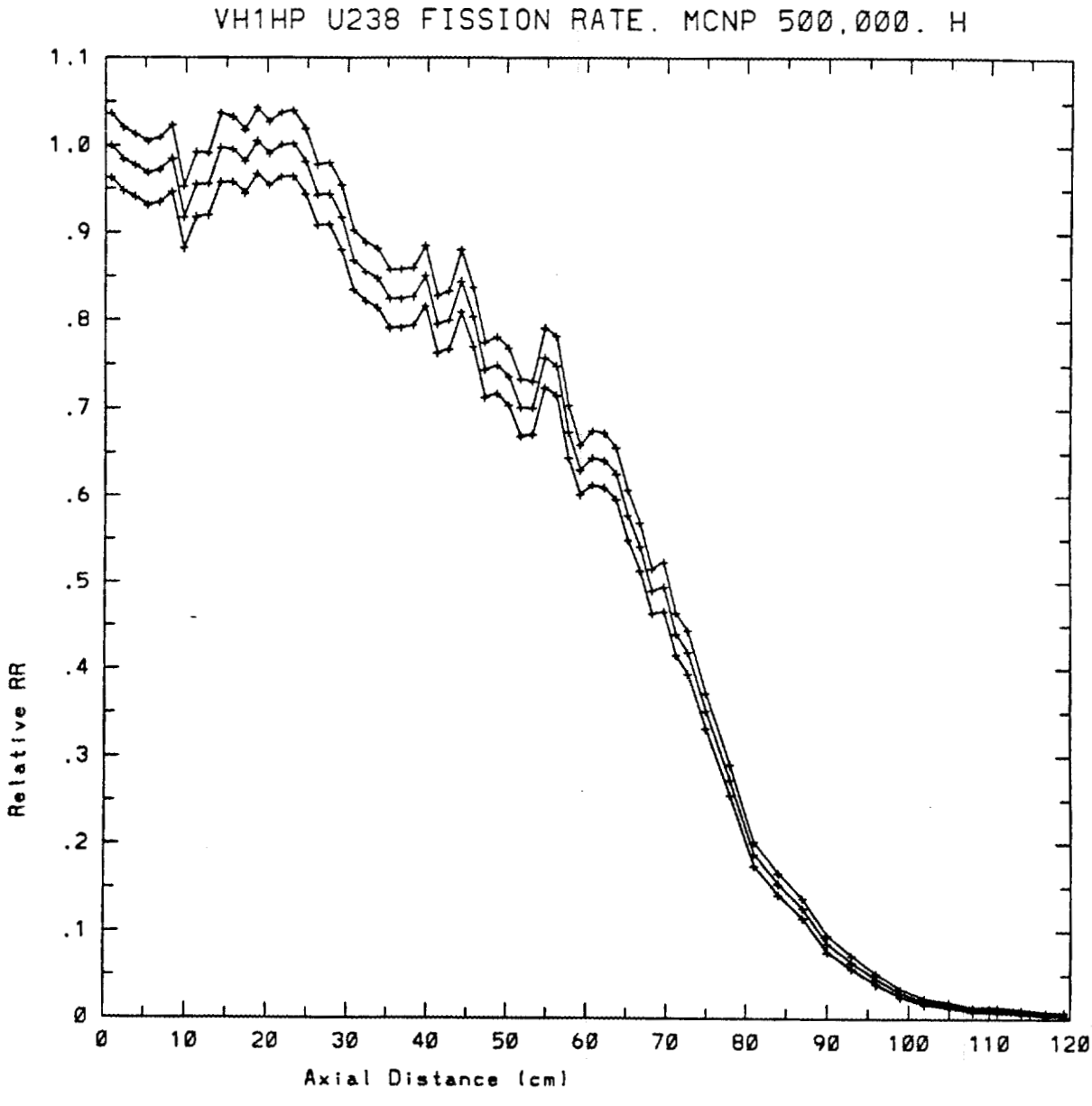

Fig. 3. ^{238}U fission rates along the z-axis, extreme curves show the uncertainties (1 sigma).

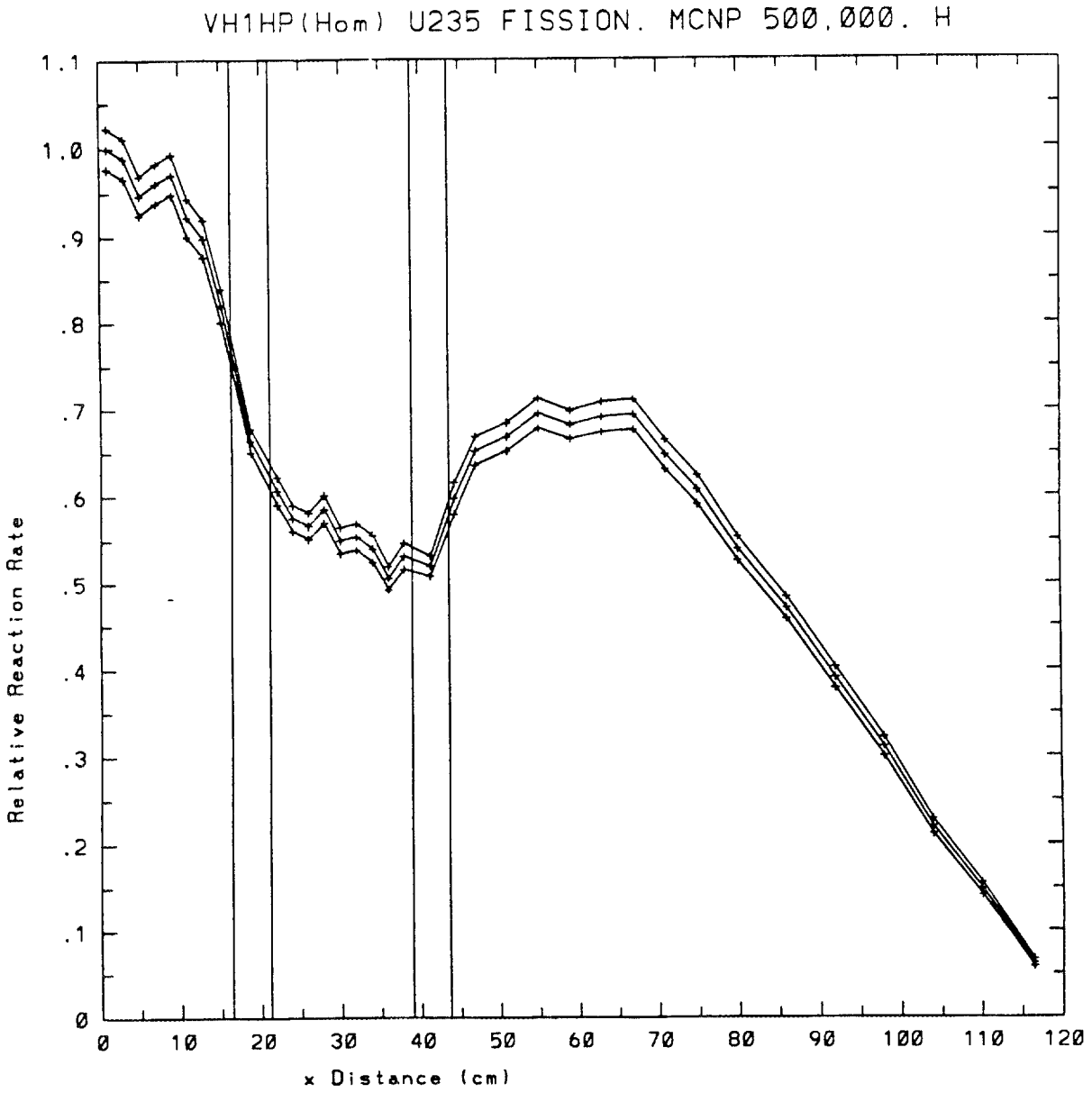

Fig. 4. ^{235}U fission rates along the x-axis, extreme curves show the uncertainties (1 sigma). The vertical lines indicate the two fuel rods crossed in this direction.

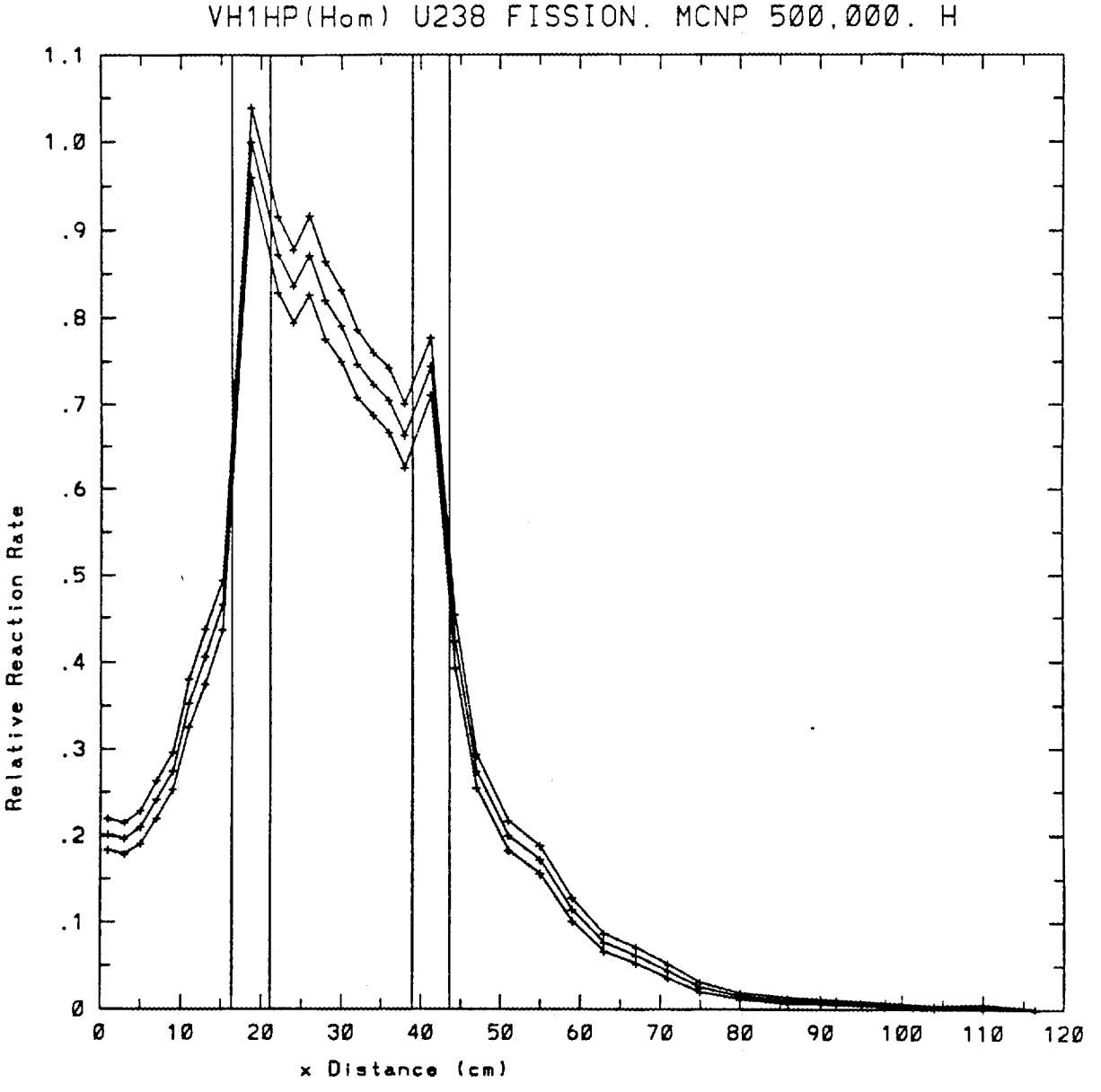

Fig. 5. ^{238}U fission rates along the x-axis, extreme curves show the uncertainties (1 sigma). The vertical lines indicate the two fuel rods crossed in this direction.

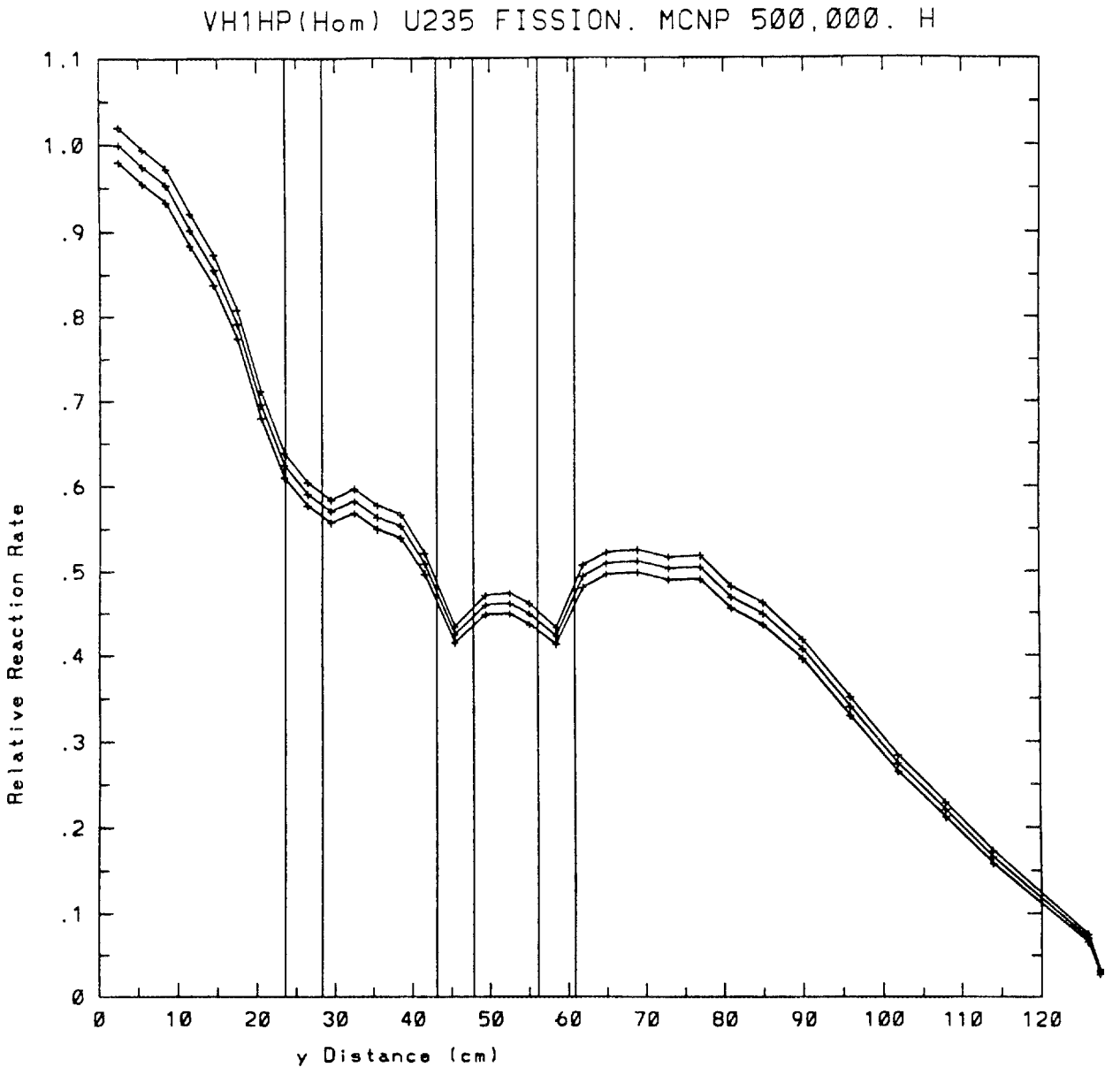

Fig. 6. ^{235}U fission rates along the y-axis, the extreme curves show the uncertainties (1 sigma). The vertical lines indicate the fuel rods near (the one at ~ 25 cm) or crossed (the other two) in this direction.

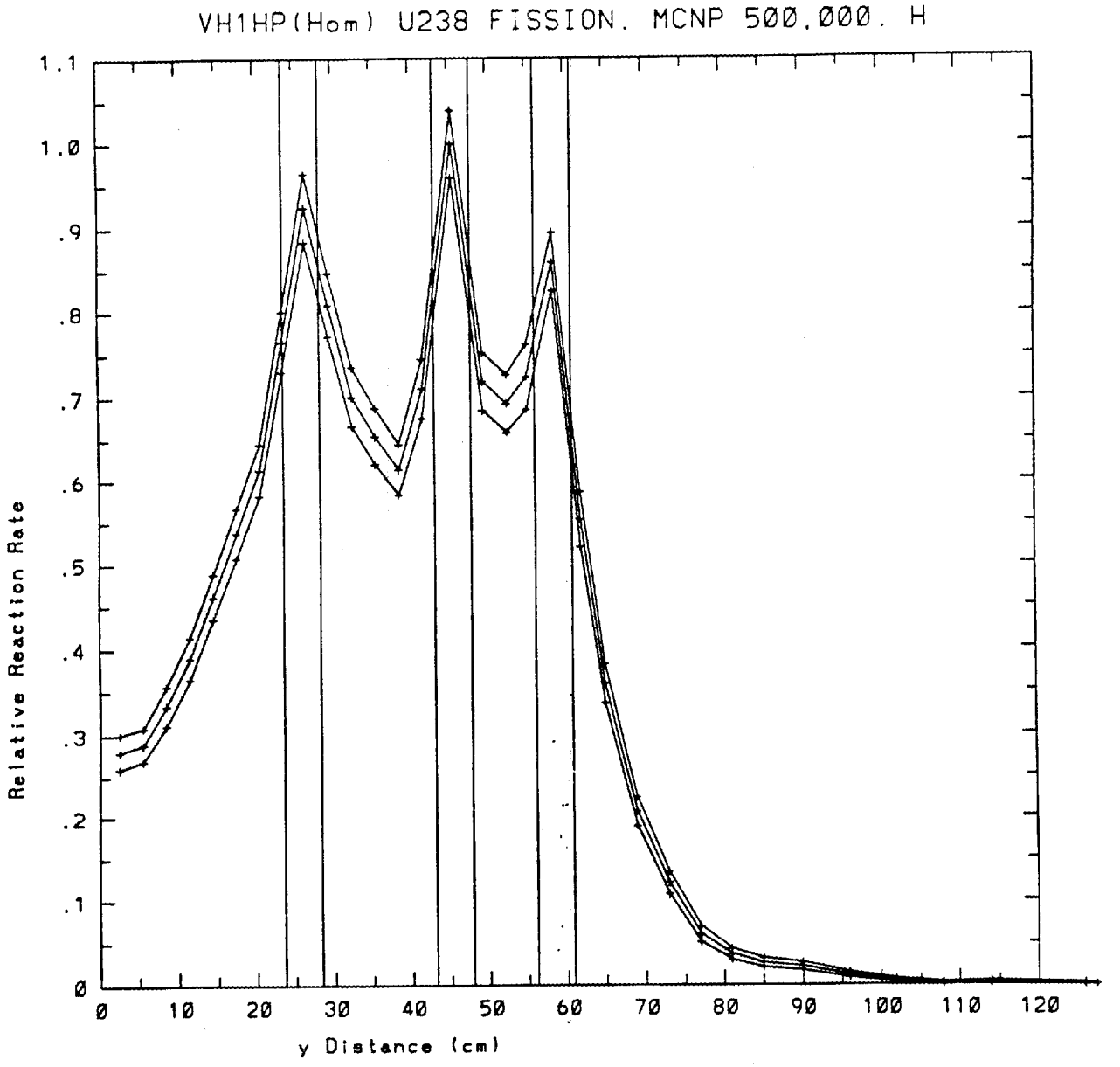

Fig. 7. ^{238}U fission rates along the *y*-axis, the extreme curves show the uncertainties (1 sigma). The vertical lines indicate the fuel rods near (the one at ~ 25 cm) or crossed (the other two) in this direction.

Table 8. Whole reactor calculators. Spectral indices[a] at the center of the core for the heterogeneous compact model

Spectral index	Value (% error)
ρ^{28}	2.054 (4.3%)
δ^{25}	0.05594 (2.5%)
δ^{28}	0.005886 (2.7%)
C*	0.3383 (3.3%)

[a] Values correspond to reaction rates in regions where the isotopes are present in the region (i.e., the fuel particles).

3. RESULTS FOR THE CALCULATION OF THE EFFECTIVE DELAYED NEUTRON FRACTION FOR THE WHOLE REACTOR

One of the requests of the benchmark is the calculation of the dollar unit, the effective delayed neutron fraction, this can be done with MCNP because it has the capability to calculate the response of the system to the injection of a pulse of neutrons. The time dependent reaction rate can then be fit to an exponential decay to determine the prompt decay constant α, which is related to the multiplication factor, k by the inhour equation:

$$\rho = \alpha \Lambda - \beta f(\alpha) \tag{1}$$

where ρ is the reactivity in absolute units, $\rho = (1-k)/k$, $\Lambda = \ell/k$ is the generation time, Λ and β are effective values,

$$f(\alpha) = \alpha \sum_{i=1}^{6} \frac{a_i}{\alpha - \lambda_i} \tag{2}$$

and a_i are the relative production of neutrons for delayed group i. If, for two states with equal ℓ/k, we compute ρ and α, β and Λ can be obtained from Eq. (1). If more states are available, a fit of Eq. (1) would improve the accuracy. The condition for this method is to calculate states with equal ℓ/k, condition that can be checked because MCNP makes also an estimation of the mean life of the neutrons ℓ.

Because of its simplicity and fast spectra, the Godiva configuration was chosen to test this method for the calculation β. The short lifetime of the neutrons makes the MCNP run particularly fast.

Static (for ρ) and pulsed neutron source (PNS) (for α) runs were made for the GODIVA configuration with different radius listed in Table 9 (which includes also typical CPU times).

Table 9. Static and PNS runs for GODIVA

Radius (cm)	Static		PNS	
	Histories	CPU (min)	Histories	CPU (min)
8.0	800,000.0	14.0	100,000.0	86.0
8.5	800,000.0	15.0	100,000.0	317.0
8.62	800,000.0	16.0	100,000.0	553.0

The reactivity was changed by changing the radius with the results summarized in Table 10.

Table 10. Results for GODIVA

Radius (cm)	k	ℓ (nsec)	ℓ/k (nsec)
8.0	0.92570 ± 0.00075	5.20 ± 0.01	5.62
8.5	0.97405 ± 0.00066	5.52 ± 0.01	5.67
8.62	0.98610 ± 0.00068	5.61 ± 0.01	5.69

Table 10 shows that Λ is fairly constant for this example. Note that the ℓ of Table 9 is an estimator computed by MCNP by following the fate of the neutrons while the ℓ and Λ of Eq. (1) are averages weighted with static adjoint fluxes; although very useful to check the constancy of Λ, the ℓ from MCNP calculations do not have to be confused with the kinetic ℓ of Eq. (1).

With the ρ of Table 10 and the α's from the fit of the PNS runs we have the results of Table 11.

Table 11. ρ and α for GODIVA

R (cm)	ρ (% error)	α (sec^{-1})
8.0	0.080264 (1.1)	$16,418,460.0 \pm 47191.0$
8.5	0.026641 (2.6)	$6,172,705.0 \pm 13143.0$
8.62	0.014096 (5.0)	$3,939,115.0 \pm 8757.0$

Note that the method relies on the calculation of ρ whose errors are difficult to reduce when the system approaches criticality. With the values of Table 11 and considering that for GODIVA $f(\alpha)$ in Eq. (1) is equal to 1, Λ and β can be determined by a linear square fit; results are in Table 12.

Table 12. Determination of Λ and β for GODIVA

Λ = (5.284 ± 0.087) nsec	(1.6%)
β = 0.00638 ± 0.00080	(12.5%)
$\alpha_g = \frac{\beta}{\Lambda}$ = 1, 207,975 ± 168,718	(14.0%)

For this case, the inverse of the effective generation time (α_g) is equal to the prompt decay constant at delay critical. The value for β is smaller than the nuclear β, result we should expect for this fast system; statistical errors are, anyway, large and mainly reflect the large errors of ρ near critical.

Some preliminary calculations were done to apply this technique for the VH1-HP benchmark. The reactivity was changed by changing the amount of equivalent ^{10}B impurities in the graphite outside the fuel rods; the nominal ^{10}B impurities in the calculations of Table 6 is 1.54 ppm (^{10}B atoms per million atoms in the mixture). This number was increased by a factor of 20 with the results shown in Table 13.

Table 13. VH1-HP whole reactor. Effect of changing ^{10}B concentration.
Results from heterogeneous compact calculations

C = ^{10}B concentration (ppm) in graphite	k
1.54 (nominal)	1.01131 ± 0.00110
30.80 (20 times nominal)	0.98382 ± 0.00374
$\Delta k/\Delta C$ = -93.9 pcm/ppm (1 pcm = Δ k*100,000.0)	

The pulsed neutron source experiment was simulated then for the subcritical system of Table 13 (i.e., including fuel particles explicitly) with the results shown in Fig. 8. The fit of this data gives α = (14.24 ± 0.67) sec^{-1}. Because MCNP mimics the fate of the neutrons in the real reactor, the calculations of the PNS experiment are particularly slow for graphite reactors near critical; for this 1.6% subcritical case it was required 8.8 days of the CPU time of an IBM workstation to compute the time profile.

4. COMPARISON WITH OTHER CALCULATIONS

Similar calculations were made by other laboratories, namely General Atomic (GA) in the U.S., Japan Energy Research Institute (JAERI), and the Kurchatov Institute in Russia. The results were obtained from Ref. 2 and compared here with our calculations.

Table 14 shows the values for the critical parameters of the 4% enriched VH1-HP cell. Tables 15 and 16 show reaction rates for the cell materials, Table 17 for the spectral indices, and Table 18 values for whole reactor calculations. Our discrepancy with the measured k is +0.35% very similar to the average discrepancy quoted by GA in Ref. 2.

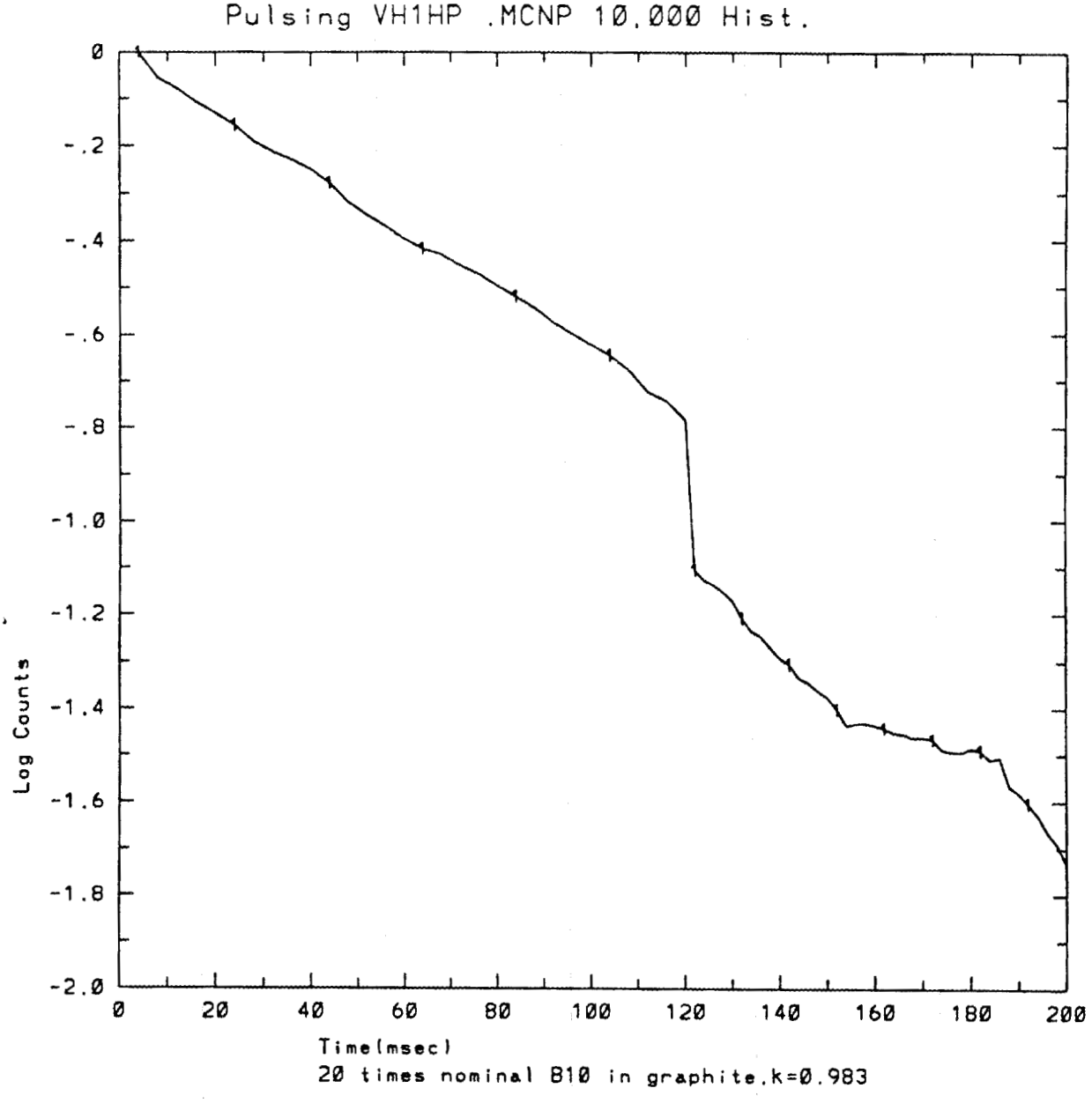

Fig. 8. VH1-HP configuration with 20 times the nominal ^{10}B concentration in the graphite; results of the simulation of a pulsed neutron experiment. Note at 120 msec the reduction, by a factor of 2, of the channel width Δt.

Table 14. Intercomparison of cell parameter for VH1-HP

Parameter	This work[a]	GA[b]	JAERI[b]
$k_\infty(B^2=0)$	1.50159 ± 0.00305	1.5069	1.4944
$B_c^2(m^{-2})$	7.836 ± 0.100	8.443	8.108
$k_\infty(B_c^2)$	1.44401 ± 0.00401	1.4548	1.4436
$M^2(cm^2)$	566.640 ± 8.812	538.6	547.1

[a]From Table 2, T=26.85°C (300°K).
[b]Values were interpolated for T=26.85°C.

Table 15. Intercomparison of capture rates in cell calculations for VH1-HP

Nuclide	This work[a]	GA[b]	JAERI[b]
^{234}U	1.261-3	1.551-3	1.420-3
^{235}U	1.145-1 (0.5%)	1.158-1	1.154-1
^{236}U	3.0374-4	3.433-4	3.345-4
^{238}U	2.518-1 (0.5%)	2.467-1	2.471-1
^{1}H	4.447-4	4.256-4	4.336-4
^{10}B	7.267-4	7.327-4	7.394-4
^{12}C	3.597-2 (1.2%)	3.506-2	3.557-2
^{14}N	2.264-3	2.616-3	2.631-3
^{16}O	2.188-4	2.061-4	1.990-4

[a]At T=26.85°C and from Table 3, some statistical error shown.
[b]At T=25.5°C (corrections for ΔT are negligible).

Table 16. Intercomparison of fission rates in cell calculations for VH1-HP

Nuclide	This work[a]	GA[b]	JAERI[b]
^{234}U	2.048-5 (6%)	1.167-5	7.025-6
^{235}U	5.882-1 (0.2%)	5.926-1	5.920-1
^{236}U	3.887-6	6.512-6	2.294-6
^{238}U	4.226-3 (7%)	3.913-3	4.218-3

[a]From Table 3, at T=26.85°C. Some statistical error shown.
[b]At T=25.5°C (corrections for ΔT are negligible).

Table 17. Intercomparison of spectral indices in cell calculation for VH1-HP

Parameter	This work[a]	GA[b]	JAERI[b]
ρ^{28}	2.980	2.776	2.823
δ^{25}	0.07698	0.07232	0.07464
δ^{28} (macro)	0.007061	0.006604	0.007128
C* (macro)	0.4356	0.4164	0.4173

[a] From Table 4 at T=26.85°C. Reaction rates only in those regions where isotopes are present (i.e., fuel particles), statistical error is 1%.
[b] At T=25.5°C (corrections for ΔT are negligible).

Table 18. Intercomparison of whole reactor k for VH1-HP at T=25.5°C

Experiment	1.008
This work[a]	1.01154 ± 0.00110
GA	1.0134
JAERI	1.0162
KI	1.0167

[a] From Table 6 and temperature coefficient -1.73 x 10^{-4}/°C (experimental).

5. CONCLUSIONS AND RECOMMENDATIONS

MCNP calculations of the VHTRC benchmark allow unprecedented degree of details in the models not available with other methods. The reactor was modeled in all of its details from the fuel particles (502 microns diameter) to the reflector (2.4 m flat to flat) and with continuous energy representation of the cross sections. Details like the end caps of the fuel rods can be modeled exactly with the flexibility of MCNP.

All the requested parameters from the specifications of the benchmarks can be calculated. In addition, pulsed neutron experiments (usual technique at PROTEUS and VHTRC facilities) can be modeled explicitly, so MCNP is going to play a major role in the interpretation of experiments to determine the impurities of the graphite and reactivities. Our results compare very well with respect to the calculations of three independent groups.

The model can be easily improved by the introduction of more details about experimental devices. Required CPU times are large; in a good proportion this is due to the long lifetime of the neutrons in the graphite system, the problem is particularly severe when PNS experiments near critical are simulated. It is strongly recommended then to use the high performance computer resources at ORNL to take advantage of the flexibility of MCNP to work with parallel computers.

REFERENCES

1. H. Yasuda, T. Yamana, and K. Tsuchihashi, "VHTRC Temperature Coefficient Benchmark Problem," presented to the *Second Research Coordination Meeting*, JAERI-Tokai, May 20-22, 1991.

2. M. Schmidt-Hoenow and R. A. Rucker, "Analysis of VHTRC Physics Benchmarks," General Atomics DOE-HTGR-90363, Revision 0 (May 1993).

Appendix A

FISSION RATES OF ^{235}U AND ^{238}U ALONG THE COORDINATES AXIS

Table A.1. VH1HP (homogeneous compact) ^{235}U fission. MCNP 500,000. HIST x-axis profile

x (cm)	Fission rate	Relative error
1.00	7.77230E-02	0.0227
3.00	7.68734E-02	0.0225
5.00	7.36861E-02	0.0231
7.00	7.47202E-02	0.0229
9.00	7.54846E-02	0.0228
11.00	7.17033E-02	0.0237
13.00	6.97792E-02	0.0238
15.19	6.37887E-02	0.0231
18.74	5.16741E-02	0.0204
22.05	4.71847E-02	0.0255
24.00	4.48024E-02	0.0252
26.00	4.41325E-02	0.0264
28.00	4.55902E-02	0.0268
30.00	4.28101E-02	0.0268
32.00	4.31248E-02	0.0270
34.00	4.20833E-02	0.0287
36.00	3.94038E-02	0.0265
37.94	4.13992E-02	0.0284
41.26	4.04939E-02	0.0226
44.31	4.64662E-02	0.0293
47.00	5.07035E-02	0.0250
51.00	5.19617E-02	0.0241
55.00	5.40387E-02	0.0245
59.00	5.30020E-02	0.0239
63.00	5.36868E-02	0.0251
67.00	5.39071E-02	0.0250
71.00	5.03547E-02	0.0261
75.00	4.72485E-02	0.0270
80.00	4.20110E-02	0.0256
86.00	3.66390E-02	0.0277
92.00	3.03791E-02	0.0305
98.00	2.41918E-02	0.0353
104.00	1.70889E-02	0.0383
110.00	1.15747E-02	0.0469
116.45	4.86974E-02	0.0669

Table A.2. VH1HP (homogeneous compact) ^{235}U fission. MCNP 500,000. HIST y-axis profile.

y (cm)	Fission rate	Relative error
2.5	7.79966E-02	0.0200
5.5	7.60279E-02	0.0203
8.5	7.43555E-02	0.0203
11.5	7.04089E-02	0.0206
14.5	6.67824E-02	0.0207
17.5	6.17524E-02	0.0216
20.5	5.43221E-02	0.0227
23.5	4.87779E-02	0.0229
26.5	4.61513E-02	0.0230
29.5	4.45498E-02	0.0235
32.5	4.54822E-02	0.0242
35.5	4.39922E-02	0.0250
38.5	4.31814E-02	0.0248
41.55	3.97484E-02	0.0242
45.46	3.31747E-02	0.0223
49.41	3.59088E-02	0.0249
52.5	3.60592E-02	0.0266
55.05	3.50668E-02	0.0276
58.46	3.30115E-02	0.0233
61.91	3.85681E-02	0.0274
65.00	3.97756E-02	0.0253
69.00	3.99613E-02	0.0260
73.00	3.92755E-02	0.0265
77.00	3.93843E-02	0.0278
81.00	3.66123E-02	0.0280
85.00	3.50674E-02	0.0295
90.00	3.17828E-02	0.0280
96.00	2.65791E-02	0.0312
102.00	2.14099E-02	0.0356
108.00	1.72037E-02	0.0380
114.00	1.29204E-02	0.0456
126.00	5.56480E-03	0.0663
132.00	2.41523E-03	0.0867

Table A.3. VH1HP (heterogeneous compact) ^{235}U fission. MCNP 500,000. HIST axial profile.

z (cm)	Fission rate	Relative error
0.75	6.78371E-02	0.0140
2.25	6.72653E-02	0.0143
3.75	6.75469E-02	0.0142
5.25	6.82225E-02	0.0142
6.75	6.83139E-02	0.0143
8.25	6.84058E-02	0.0141
9.75	6.78376E-02	0.0141
11.25	6.72440E-02	0.0140
12.75	6.76112E-02	0.0143
14.25	6.74218E-02	0.0145
15.75	6.67166E-02	0.0142
17.25	6.69589E-02	0.0144
18.75	6.67600E-02	0.0144
20.25	6.60304E-02	0.0144
21.75	6.47906E-02	0.0144
23.25	6.41855E-02	0.0146
24.75	6.47748E-02	0.0147
26.25	6.46810E-02	0.0146
27.75	6.38619E-02	0.0145
29.25	6.30352E-02	0.0147
30.75	6.22337E-02	0.0148
32.25	6.15721E-02	0.0147
33.75	5.98740E-02	0.0147
35.25	6.00415E-02	0.0151
36.75	6.01952E-02	0.0151
38.25	5.96082E-02	0.0153
39.75	5.83975E-02	0.0152
41.25	5.74562E-02	0.0156
42.75	5.65063E-02	0.0154
44.25	5.60777E-02	0.0155
45.75	5.59461E-02	0.0157
47.25	5.40796E-02	0.0157
48.75	5.31815E-02	0.0159
50.25	5.25364E-02	0.0163
51.75	5.18652E-02	0.0160
53.25	5.10211E-02	0.0163
54.75	5.09167E-02	0.0170

Table A.3. VH1HP (heterogeneous compact) ^{235}U fission. MCNP 500,000. HIST axial profile.

z (cm)	Fission rate	Relative error
56.25	5.06113E-02	0.0171
57.75	4.95168E-02	0.0169
59.25	4.96408E-02	0.0177
60.75	4.88955E-02	0.0173
62.25	4.71760E-02	0.0173
63.75	4.58272E-02	0.0174
65.25	4.44730E-02	0.0176
66.75	4.39581E-02	0.0176
68.25	4.26645E-02	0.0177
69.75	4.16747E-02	0.0178
71.25	4.27666E-02	0.0180
72.75	4.23654E-02	0.0179
75.00	4.16756E-02	0.0177
78.00	4.15552E-02	0.0181
81.00	4.00424E-02	0.0183
84.00	3.90871E-02	0.0193
87.00	3.71807E-02	0.0198
90.00	3.40156E-02	0.0207
93.00	3.11369E-02	0.0217
96.00	2.79430E-02	0.0226
99.00	2.52870E-02	0.0234
102.00	2.22048E-02	0.0250
105.00	1.87439E-02	0.0268
108.00	1.53175E-02	0.0285
111.00	1.23675E-02	0.0306
114.00	8.77178E-03	0.0334
117.00	5.56756E-03	0.0369
119.25	2.97103E-03	0.0420

Table A.4. VH1HP (homogeneous compact) ^{238}U fission. MCNP 500,000. HIST x-axis profile.

x(cm)	Fission rate	Relative error
1.0	2.16610E-06	0.0902
3.0	2.11282E-06	0.0921
5.0	2.25633E-06	0.0900
7.0	2.60066E-06	0.0909
9.0	2.95846E-06	0.0801
11.0	3.80131E-06	0.0780
13.0	4.37100E-06	0.0761
15.19	5.00800E-06	0.0622
18.74	1.07624E-05	0.0394
22.05	9.39423E-06	0.0495
24.00	9.00464E-06	0.0496
26.00	9.38289E-06	0.0516
28.00	8.82929E-06	0.0537
30.00	8.51448E-06	0.0517
32.00	8.04442E-06	0.0525
34.00	7.78623E-06	0.0511
36.00	7.58052E-06	0.0542
37.94	7.13300E-06	0.0570
41.26	8.00934E-06	0.0450
44.31	4.56034E-06	0.0718
47.00	2.95582E-06	0.0703
51.00	2.15288E-06	0.0852
55.00	1.85263E-06	0.0931
59.00	1.23571E-06	0.1163
63.00	8.27568E-07	0.1324
67.00	6.67371E-07	0.1493
71.00	4.74175E-07	0.1817
75.00	2.77738E-07	0.2187
80.00	1.68260E-07	0.2280
86.00	1.11591E-07	0.3198
92.00	9.03612E-08	0.3000
98.00	6.16314E-08	0.4224
104.00	3.34294E-08	0.4949
110.00	3.69645E-08	0.8925
116.45	5.40072E-09	0.9890

Table A.5. VH1HP (homogeneous compact ^{238}U fission. MCNP 500,000. HIST y-axis profile.

y(cm)	Fission rate	Relative error
2.5	2.37788E-06	0.0728
5.5	2.45340E-06	0.0683
8.5	2.83475E-06	0.0673
11.5	3.0193E-06	0.0631
14.5	3.91712E-06	0.0578
17.5	4.55584E-06	0.0551
20.5	5.20525E-06	0.0514
23.5	6.49424E-06	0.0463
26.5	7.83407E-06	0.0436
29.5	6.86998E-06	0.0465
32.5	5.94661E-06	0.0492
35.5	5.55016E-06	0.0514
38.5	5.20821E-06	0.0507
41.55	6.02805E-06	0.0486
45.46	8.48029E-06	0.0401
49.41	6.09846E-06	0.0474
52.5	5.87319E-06	0.0489
55.05	6.13828E-06	0.0528
58.46	7.29245E-06	0.0399
61.91	4.68977E-06	0.0593
65.00	3.04277E-06	0.0623
69.00	1.75456E-06	0.0850
73.00	1.02544E-06	0.1104
77.00	5.10828E-07	0.1583
81.00	3.10324E-07	0.1788
85.00	2.23415E-07	0.2073
90.00	1.86798E-07	0.2185
96.00	9.94652E-08	0.2774
102.00	4.30515E-08	0.4616
108.00	1.61427E-08	0.5570
114.00	2.35496E-08	0.6926
126.00	7.18547E-09	0.9880
132.00	2.37996E-11	0.0944

Table A.6. VH1HP (heterogeneous compact) ^{238}U fission. MCNP 500,000. HIST axial profile.

z(cm)	Fission rate	Relative error
0.75	3.36802E-06	0.0374
2.25	3.31456E-06	0.0372
3.75	3.28998E-06	0.0369
5.25	3.26072E-06	0.0381
6.75	3.27366E-06	0.0384
8.25	3.31738E-06	0.0390
9.75	3.09068E-06	0.0379
11.25	3.21615E-06	0.0391
12.75	3.21863E-06	0.0371
14.25	3.36033E-06	0.0400
15.75	3.35361E-06	0.0380
17.25	3.30714E-06	0.0372
18.75	3.38627E-06	0.0377
20.25	3.33761E-06	0.0374
21.75	3.37182E-06	0.0372
23.25	3.37648E-06	0.0381
24.75	3.30628E-06	0.0385
26.25	3.17590E-06	0.0371
27.75	3.18046E-06	0.0380
29.25	3.08967E-06	0.0402
30.75	2.92690E-06	0.0388
32.25	2.88295E-06	0.0391
33.75	2.85858E-06	0.0400
35.25	2.77913E-06	0.0406
36.75	2.77993E-06	0.0405
38.25	2.78669E-06	0.0401
39.75	2.86637E-06	0.0406
41.25	2.68017E-06	0.0414
42.75	2.69528E-06	0.0417
44.25	2.84625E-06	0.0428
45.75	2.70738E-06	0.0420
47.25	2.50395E-06	0.0418
48.75	2.5209E-06	0.0430
50.25	2.47725E-06	0.0441
51.75	2.35899E-06	0.0455
53.25	2.35791E-06	0.0426
54.75	2.54923E-06	0.0447
56.25	2.51891E-06	0.0449
57.75	2.26862E-06	0.0440
59.25	2.12122E-06	0.0451
60.75	2.16798E-06	0.0484

Table A.6. VH1HP (heterogeneous compact) ^{238}U fission. MCNP 500,000. HIST axial profile.

z(cm)	Fission rate	Relative error
62.25	2.15845E-06	0.0491
63.75	2.10723E-06	0.0478
65.25	1.94530E-06	0.0500
66.75	1.82368E-06	0.0512
68.25	1.65011E-06	0.0525
69.75	1.66691E-06	0.0578
71.25	1.48258E-06	0.0556
72.75	1.41074E-06	0.0596
75.00	1.18372E-06	0.0575
78.00	9.20175E-07	0.0637
81.00	6.33224E-07	0.0730
84.00	5.17586E-07	0.0811
87.00	4.24860E-07	0.0881
90.00	2.90078E-07	0.1109
93.00	2.18486E-07	0.1156
96.00	1.54131E-07	0.1287
99.00	1.00053E-07	0.1518
102.00	6.72258E-08	0.1804
105.00	5.46317E-08	0.2032
108.00	3.69207E-08	0.2383
111.00	3.63428E-08	0.2775
114.00	2.95006E-08	0.3151
117.00	2.06862E-08	0.3709
119.25	1.96888E-08	0.3930

INTERNAL DISTRIBUTION

1. S. J. Ball
2-6. F. C. Difilippo
7. D. T. Ingersoll
8. S. Martin
9. G. E. Michaels
10. C. E. Oliver
11. C. E. Pugh
12. J. P. Renier
13. P. L. Rittenhouse
14. R. C. Ward
15-19. B. A. Worley
20. EPMD Reports Office
21-22. Laboratory Records Department
23. Laboratory Records, ORNL-RC
24. Document Reference Section
25. Central Research Library
26. ORNL Patent Section

EXTERNAL DISTRIBUTION

27. L. D. Mears, Gas Cooled Reactor Associates, 10240 Sorrento Valley Road, Suite 300, San Diego, CA 92121-1605.
28. G. C. Bramblett, GT-MHR Project Division, P.O. Box 85608, San Diego, CA 92186-9784.
29. D. Pettycord, GT-MHR Plant Design, Control Office-West, c/o General Atomics, P.O. Box 85608, San Diego, CA 92186-9784.
30. B. Demars, U.S. Department of Energy, Naval Reactors Office (NE-60), 3N06/NR Crystal City, Arlington, VA 22202.
31. P. M. Williams, Office of Nuclear Energy, U.S. Department of Energy, NE-42/GTN, Washington, DC 20585.
32. S. A. Caspersson, ABB/CENP, M/S 9354-0422, 1000 Prospect Hill Road, Windsor, CT 06095-0500
33. R. R. Mills, PDCO-East, 3206 Tower Oaks Blvd., Suite #300, Rockville, MD 20852-4220.
34. S. K. Ghose, Bechtel National Laboratory, P.O. Box 193965, I507, San Francisco, CA 94119.
35. W. J. Parker, Stone & Webster Engineering, 245 Summer Street, P.O. Box 2325, Boston, MA 02107.

32-34. Office of Scientific and Technical Information, U.S. Department of Energy, P.O. Box 62, Oak Ridge, TN 37831.

35. GT-MHR Plant Design, Control Office-East, Attention: R. R. Mills, MEREX, Inc., 3206 Tower Oaks Boulevard #300, Rockville, MD 20852.
36. P. J. Karcz, Office of Nuclear Energy, U.S. Department of Energy, NE-42/GTN, Germantown, MD 20585.
37. D. J. Krommenhoek, Knolls Atomic Power Laboratory, Bldg. D-2, Rm. 121, P.O. Box 1072, Schenectady, NY 12301.
38. R. Brogli, Paul Scherrer Institute, Wurenlingen und Villigen, CH-5232 Villigen PSI, Switzerland.
39. J. C. Cleveland, International Atomic Energy Agency, POB 100, A-1400, Vienna, Austria.
40. R. W. Brockett, Harvard University, Pierce Hall, 29 Oxford Street, Cambridge, MA 02138.
41. D. J. Dudziak, Department of Nuclear Engineering, 110B Burlington Engineering Labs, North Carolina State University, Raleigh, NC 27695-7909.
42. J. E. Leiss, Rt. 2, Box 142C, Broadway, VA 22815.
43. N. Moray, Department of Mechanical and Industrial Engineering, University of Illinois, 1206 West Green Street, Urbana, IL 61801.
44. M. F. Wheeler, Department of Mathematics, Rice University, P.O. Box 1892, Houston, TX 77251.
45. Office of Assistant Manager for Energy Research and Development, Department of Energy, Oak Ridge Operations Office, P.O. Box 2008, Oak Ridge, TN 37831.